

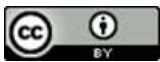
Effect of Different Parameters on Powell-Eyring Fluid Peristaltic Flow with the Influence of a Rotation and Heat Transform in an Inclined Asymmetric Channel

Rana Ghazi Ibraheem*, Liqaa Zeki Hummady

Department of Mathematics, College of Science, University of Baghdad, Baghdad, Iraq

*Corresponding Author.

Received 12/01/2023, Revised 20/03/2023, Accepted 22/03/2023, Published Online First 20/09/2023,
Published 01/04/2024



© 2022 The Author(s). Published by College of Science for Women, University of Baghdad.

This is an Open Access article distributed under the terms of the [Creative Commons Attribution 4.0 International License](https://creativecommons.org/licenses/by/4.0/), which permits unrestricted use, distribution, and reproduction in any medium, provided the original work is properly cited.

Abstract

In this article, the effect of the rotation variable and other variables on the peristaltic flow of Powell-Eyring fluid in an inclined asymmetric channel with an inclining magnetic field through a porous medium with heat transfer is examined. Long wavelength and low Reynolds number are assumed, where the perturbation approach is used to solve the nonlinear governing equations in the Cartesian coordinate system to produce series solutions. distributions of velocity and pressure gradients are expressed mathematically. Through the collection of figures, the impact of various criteria is explained and graphically represented. These numerical results were attained using the mathematical application MATHEMATICA.

Keywords: Heat transfer, Inclined channel, Magnetic field, Peristaltic flow, Porous medium, Powell-Eyring fluid, Rotation.

Introduction

Peristaltic pumping is a specific sort of pumping when a wide range of intricate rheological fluids can be moved readily from between two locations. This pumping principle is referred to as peristaltic. The ducts through which the fluid passes undergo intermittent involuntary constriction and then expand. As a result, the pressure gradient rises, causing the fluid to move forward. After Latham's groundbreaking work¹ and due to the fact that it is utilized in biological, engineering, and physiological systems academics have become increasingly interested in the different applications of peristalsis. Due to the fact that it is utilized in biological, engineering, and physiological systems, peristaltic transport has received significant attention in recent years. Generally, the peristaltic wave's circular contractions and the successive longitudinal contractions that occur during peristalsis are

generated by the sinuses which propagate along the fluid-containing duct. This technique is the basis for several muscular tubes, including the gastrointestinal tract, fallopian tubes, bile ducts, ureters, esophageal tubes, and others. Moreover, non-Newtonian fluids are better than numerous industrial and physiological processes that use Newtonian fluids. Among the models of non-Newtonian fluids (which can exhibit various rheological effects), that can be accessed is Paul-Eyring fluid. Although this model is more difficult mathematically than models of non-Newtonian fluids, it deserves more attention because of its distinct benefits. Numerous researchers have been interested in the Powell-Eyring fluid's peristaltic flow mechanism since it was studied by Hina and Mustafa and Hayat and Alsaedi², Hayat and Naseema and Rafiq and Fuad³, Hayat and Ahmed⁴, Hussain and Alvi and Latif and Asghar⁵, and Ali and

Liqaa ⁶. The static magnetohydrodynamic flow and heat transfer of an Eyring-Powell fluid on an expansion plate with viscous dissipation were studied and numerically explained⁷. The exchange of thermal energy between different system components is referred to as heat transfer. However, the medium's physical characteristics and the separate compartments' temperatures affect the speed. In recent years, research⁸⁻¹¹ has been conducted about studying the effect of heat transport on non-Newtonian fluids. In a tapered asymmetric channel, the issue of peristaltic transport of an incompressible non-Newtonian fluid is examined ¹². Peristalsis is used as the basis for the creation of devices such as peristaltic pumps, roller pumps, hose pumps, tube pumps, finger pumps, heart-lung machines, blood pump machines, and dialysis machines. These applications include the transportation of aggressive chemicals, high solid slurries, toxic (nuclear industries), and other materials. With regard to well-established problems of the stir of semi-conductive physiological fluids, such as blood and blood pump machines, magnetic drug forcing, and pertinent methods of human digestion, the advantage of applied magnetic field (MHD) on peristaltic efficacy is crucial. It is also helpful in treating gastroparesis, chronic constipation, and morbid obesity as well as magnetic resonance imaging (MRI), which is used to identify brain, vascular diseases, and tumors. A substance that has several tiny holes scattered throughout it is referred to as a porous medium. In riverbeds, fluid infiltration and seepage are sustained by flows over porous media. Important examples of flows through a porous material are those through the ground, water, and oil. Oil is trapped in rock formations like limestone and sandstone, which make up the majority of an oil reservoir ¹³. Natural porous media can be found in many different forms, such as sand, rye bread, wood, filters, bread loaves, human lungs, and the gallbladder. Food processing, oxygenation, hemodialysis, tissue condition, heat convection for blood flow from tissues' pores, and radiation between the environment and its surface all depend on the action of heat transfer in the peristaltic repositioning of fluid ¹⁴⁻¹⁷. The aforementioned processes all benefit from mass transfer; in particular, the mass transfer that occurs as nutrients diffuse from the blood into nearby tissues cannot be understated. Greater mass transfer participation is typical in the distillation, diffusion of chemical contaminants, membrane separation, and combustion processes. It

should be observed that when mass and heat transmission happens at the same time, there is a connection between driving potentials and fluxes. However, the temperature gradient is what causes the gradients in mass flux and composition (termed solet action). The study of fluid peristaltic transport in the presence of an external magnetic field and rotation is necessary for many issues involving the flow of conductive physiological fluids, such as blood and saline water¹⁸. A variety of values are used for the rotational parameters, the porous medium, density, amplitude wave, and taper of the channel, as well as a variety of values for the Hartman number and Darcy number, to study the effects of varying the velocity and pressure gradient. This article's objective is to look into the rotational effects of the peristaltic transport of a Powell-Eyring fluid through a porous media under the combined influence of inclined MHD.

Problem Mathematical Description

Consider the peristaltic motion of an incompressible Powell-Eyring fluid in a two-dimensional, asymmetric conduit with a width of $(d+d')$. An endless sinusoidal wave traveling along the channel walls at a constant forward speed (c) is what generates flow.

The geometry of the wall structure is described as:

$$\begin{aligned} \bar{h}_1(\bar{X}, \bar{t}) &= d - a_1 \sin \left[\frac{2\pi}{\lambda} (\bar{x} - c\bar{t}) \right] & 1 \\ \bar{h}_2(\bar{X}, \bar{t}) &= -d' - a_2 \sin \left[\frac{2\pi}{\lambda} (\bar{x} - c\bar{t}) + \Phi \right] & 2 \end{aligned}$$

In which $\bar{h}_1(\bar{x}, \bar{t})$, $\bar{h}_2(\bar{x}, \bar{t})$ are the lower and upper walls respectively, (d, d') denote the channel width, (a_1, a_2) are the amplitudes of the wave, (λ) is the wavelength, (c) is wave the wave speed, (Φ) varies in the range $(0 \leq \Phi \leq \pi)$, when $\Phi = 0$ is a symmetric channel with out-of-phase waves and $\Phi = \pi$ waves are in phase, the rectangular coordinate system is chosen so that the $\bar{X} - axis$ is in the direction of the wave's motion. and the $\bar{Y} - axis$ perpendicular to \bar{X} , where \bar{t} is the time as shown in **Error! Reference source not found.**

Further a_1, a_2, d, d' and Φ fulfill the following condition;

$$a_1^2 + a_2^2 + 2a_1a_2 \cos \Phi \leq (d + d')^2 \quad 3$$

The Cauchy stress tensor $\bar{\tau}$ for a fluid that obeys the Powell- Eyring model is given as follows:-

$$\bar{\tau} = -PI + \bar{S} \quad 4$$

$$\bar{S} = \left[\mu + \frac{1}{\beta \gamma} \sinh^{-1} \left(\frac{\dot{\gamma}}{c_1} \right) \right] A_{11} \quad 5$$

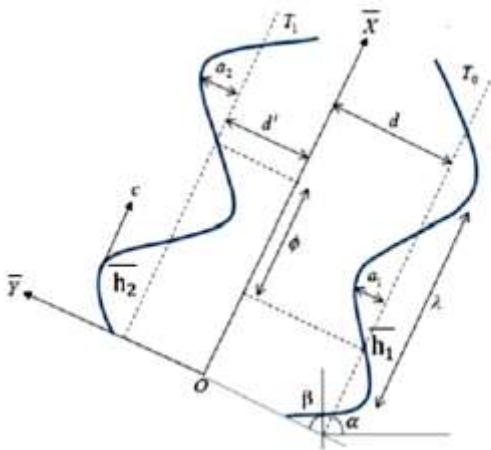


Figure 1. Coordinates for Inclined Asymmetric Channels in Cartesian Space

$$\dot{\gamma} = \sqrt{\frac{1}{2} \text{tr}(A_{11})^2} \quad 6$$

$$A_{11} = \nabla \bar{V} + (\nabla \bar{V})^T \quad 7$$

Where \bar{S} is the extra stress tensor, I is the identity tensor, $\nabla = (\partial \bar{X}, \partial \bar{Y}, 0)$ is the gradient vector, (β, c_1) are the material parameters of Powell-Eyring fluid, P is the fluid pressure, and μ the dynamic viscosity. The term \sinh^{-1} is approximately equivalent to

$$\sinh^{-1} \left(\frac{\dot{\gamma}}{c_1} \right) = \frac{\dot{\gamma}}{c_1} - \frac{\dot{\gamma}^3}{6c_1^3}, \quad \left| \frac{\dot{\gamma}^5}{6c_1^5} \right| \ll 1 \quad 8$$

The flow is governed by three coupled nonlinear partial differentials of continuity, momentum, and energy, which are expressed in frame (\bar{X}, \bar{Y}) as

$$\frac{\partial \bar{U}}{\partial \bar{X}} + \frac{\partial \bar{V}}{\partial \bar{Y}} = 0 \quad 9$$

$$\begin{aligned} \rho \left(\frac{\partial \bar{U}}{\partial \bar{t}} + \bar{U} \frac{\partial \bar{U}}{\partial \bar{X}} + \bar{V} \frac{\partial \bar{U}}{\partial \bar{Y}} \right) - \rho \Omega \left(\Omega \bar{U} + 2 \frac{\partial \bar{V}}{\partial \bar{t}} \right) = \\ - \frac{\partial \bar{P}}{\partial \bar{X}} + \frac{\partial \bar{S}_{\bar{X}\bar{X}}}{\partial \bar{X}} + \frac{\partial \bar{S}_{\bar{X}\bar{Y}}}{\partial \bar{Y}} - \sigma \beta_0^2 \cos \beta (\bar{U} \cos \beta - \\ \bar{V} \sin \beta) \\ - \frac{\mu}{k} \bar{U} + p g \sin \alpha^* \end{aligned} \quad 10$$

Where ρ is the fluid density, $\bar{V} = [\bar{U}, \bar{V}]$ is the velocity vector, \bar{P} is the hydrodynamic pressure, $\bar{S}_{\bar{X}\bar{X}}, \bar{S}_{\bar{X}\bar{Y}},$ and $\bar{S}_{\bar{Y}\bar{Y}}$ are the elements of the extra stress tensor \bar{S} , σ is the electrical conductivity, β_0 is the constant magnetic field, β is the inclination of the magnetic field, Ω is the rotation C_p is specific heat, k' is the thermal conductivity, \bar{T} is a temperature, and μ for viscosity.

Listed below are the parts of Powell-additional Eyring's stress tensor, as described by Eq.5

$$\begin{aligned} \rho \left(\frac{\partial \bar{V}}{\partial \bar{t}} + \bar{U} \frac{\partial \bar{V}}{\partial \bar{X}} + \bar{V} \frac{\partial \bar{V}}{\partial \bar{Y}} \right) - \rho \Omega \left(\Omega \bar{U} + 2 \frac{\partial \bar{V}}{\partial \bar{t}} \right) = \\ - \frac{\partial \bar{P}}{\partial \bar{Y}} + \frac{\partial \bar{S}_{\bar{X}\bar{Y}}}{\partial \bar{X}} + \frac{\partial \bar{S}_{\bar{Y}\bar{Y}}}{\partial \bar{Y}} - \sigma \beta_0^2 \sin \beta (\bar{U} \cos \beta - \\ \bar{V} \sin \beta) - \frac{\mu}{k} \bar{V} + p g \cos \alpha^* \end{aligned} \quad 11$$

$$\begin{aligned} \rho C_p \left(\frac{\partial \bar{T}}{\partial \bar{t}} + \bar{U} \frac{\partial \bar{T}}{\partial \bar{X}} + \bar{V} \frac{\partial \bar{T}}{\partial \bar{Y}} \right) = k' \left(\frac{\partial^2 \bar{T}}{\partial \bar{t}^2} + \frac{\partial^2 \bar{T}}{\partial \bar{X}^2} + \right. \\ \left. \frac{\partial^2 \bar{T}}{\partial \bar{Y}^2} \right) + \mu \left[\left(\frac{\partial \bar{U}}{\partial \bar{Y}} + \frac{\partial \bar{V}}{\partial \bar{X}} \right)^2 + 2 \left(\frac{\partial \bar{U}}{\partial \bar{X}} \right)^2 + 2 \left(\frac{\partial \bar{V}}{\partial \bar{Y}} \right)^2 \right] \end{aligned} \quad 12$$

$$\begin{aligned} \bar{S}_{\bar{X}\bar{X}} = 2 \left(\mu + \frac{1}{\beta c_1} \right) \bar{U}_{\bar{X}} - \frac{1}{3\beta c_1^3} \left[2\bar{U}_{\bar{X}}^2 + (\bar{V}_{\bar{X}} + \bar{U}_{\bar{Y}})^2 + 2\bar{V}_{\bar{Y}}^2 \right] \bar{U}_{\bar{X}} \end{aligned} \quad 13$$

$$\begin{aligned} \bar{S}_{\bar{X}\bar{Y}} = 2 \left(\mu + \frac{1}{\beta c_1} \right) (\bar{V}_{\bar{X}} + \bar{U}_{\bar{Y}}) - \frac{1}{6\beta c_1^3} \left[2\bar{U}_{\bar{X}}^2 + (\bar{V}_{\bar{X}} + \bar{U}_{\bar{Y}})^2 + 2\bar{V}_{\bar{Y}}^2 \right] (\bar{V}_{\bar{X}} + \bar{U}_{\bar{Y}}) \end{aligned} \quad 14$$

$$\begin{aligned} \bar{S}_{\bar{Y}\bar{Y}} = 2 \left(\mu + \frac{1}{\beta c_1} \right) \bar{V}_{\bar{Y}} - \frac{1}{3\beta c_1^3} \left[2\bar{U}_{\bar{X}}^2 + (\bar{V}_{\bar{X}} + \bar{U}_{\bar{Y}})^2 + 2\bar{V}_{\bar{Y}}^2 \right] \bar{V}_{\bar{Y}} \end{aligned} \quad 15$$

Natural peristaltic motion is an erratic occurrence, but it applying the transformation from a laboratory frame, stability can be assumed (fixed frame) (\bar{X}, \bar{Y}) to wave frame (move frame) (\bar{x}, \bar{y}) . The subsequent transformations determine the relationship between coordinates, velocities, and pressure in the laboratory frame (\bar{X}, \bar{Y}) to wave frame (\bar{x}, \bar{y})

$$\begin{aligned} \bar{x} = \bar{X} + c\bar{t}, \bar{y} = \bar{Y}, \bar{u} = \bar{U} - c, \bar{v} = \bar{V}, \bar{p}(\bar{x}, \bar{y}) = \\ \bar{P}(\bar{X}, \bar{Y}, \bar{t}) \end{aligned} \quad 16$$

Where \bar{u} and \bar{v} represent the velocity factors and \bar{p} represents the pressure in the wave frame. Now that Eq.15 has been substituted into Eqs.1, 2, and 9–14, the resulting equation has been normalized using the non-dimensional variables shown below:

$$\begin{aligned} x = \frac{1}{\lambda} \bar{x}, y = \frac{1}{d} \bar{y}, u = \frac{1}{c} \bar{u}, v = \frac{1}{\delta c} \bar{v}, P = \frac{d^2}{\lambda \mu c} \bar{p}, t = \\ \frac{c}{\lambda} \bar{t}, h_1 = \frac{1}{d} \bar{h}_1, h_2 = \frac{1}{d} \bar{h}_2, \delta = \frac{d}{\lambda}, Re = \frac{\rho c d}{\mu}, \\ Ha = d \sqrt{\frac{\sigma}{\mu}} \beta_0, Da = \frac{k}{d^2}, w = \frac{1}{\mu \beta c_1}, A = \\ \frac{w}{6} \left(\frac{c}{c_1 d} \right)^2, \bar{T} = T - T_0, \theta = \frac{T - T_0}{T_1 - T_0}, Fr = \\ \frac{c^2}{dg}, \beta_1 = \frac{\beta^*}{d}, S_{xx} = \frac{\lambda}{\mu c} \bar{S}_{\bar{X}\bar{X}}, S_{xy} = \frac{d}{\mu c} \bar{S}_{\bar{X}\bar{Y}}, d^* = \frac{d'}{d}, \end{aligned}$$



$$\mathbf{a} = \frac{a_1}{d}, \mathbf{b} = \frac{a_2}{d}, S_{yy} \frac{d}{\mu c} \bar{S}_{\bar{y}\bar{y}} \quad 17$$

Where, (δ) is the wave number, (h_1) and (h_2) are non-dimensional lower and upper wall surfaces respectively, (Re) is the Reynolds number, (Ha) is the Hartman number, (Φ) is the amplitude ratio, (w) is the non-dimensional permeability of the porous medium parameter, (Da) is the Darcy number, (A) is the Powell-Eyring fluid parameter, (T_0) and (T_1) are the temperatures at the upper and lower walls, (Fr) is the Froude number, and (α^*) the inclination angle of the channel to the horizontal axis.

Following that is

$$h_1(x) = 1 - a \sin(2\pi x) \quad 18$$

$$h_2(x) = -d^* - b \sin(2\pi x + \Phi) \quad 19$$

Where a, b, d^* , and satisfy Eq.3, then

$$a^2 + b^2 + 2ab \cos \Phi \leq (1 + d^*)^2 \quad 20$$

$$\frac{\partial u}{\partial x} + \frac{\partial v}{\partial y} = 0 \quad 21$$

$$Re \delta \left(\frac{\partial u}{\partial t} + u \frac{\partial u}{\partial x} + v \frac{\partial u}{\partial y} \right) - \frac{\rho d^2 \Omega}{\mu} \left(\Omega u + 2 \frac{\delta c}{d} \frac{\partial v}{\partial t} \right) = -\frac{\partial p}{\partial x} + \delta^2 \frac{\partial}{\partial x} S_{xx} + \frac{\partial}{\partial y} S_{xy} - Ha^2 \cos \beta (u \cos \beta - \delta v \sin \beta) - \frac{1}{Da} u + \frac{Re}{Fr} \sin \alpha^* \quad 22$$

$$Re \delta^3 \left(\frac{\partial v}{\partial t} + u \frac{\partial v}{\partial x} + v \frac{\partial v}{\partial y} \right) - \frac{\rho d^2 \Omega \delta}{\mu} \left(\Omega u + 2 \frac{\delta c}{d} \frac{\partial v}{\partial t} \right) = -\frac{\partial p}{\partial x} + \delta^2 \frac{\partial}{\partial x} S_{xy} + \delta \frac{\partial}{\partial y} S_{yy} + Ha^2 \sin \beta (\delta u \cos \beta - \delta^2 v \sin \beta) - \delta^2 \frac{1}{Da} v + \delta \frac{Re}{Fr} \cos \alpha^* \quad 23$$

$$Re \delta \left(\frac{\partial \theta}{\partial t} + u \frac{\partial \theta}{\partial x} + v \frac{\partial \theta}{\partial y} \right) = \frac{1}{Pr} \left(c^2 \delta^2 \frac{\partial^2 \theta}{\partial t^2} + \delta^2 \frac{\partial^2 \theta}{\partial x^2} + \frac{\partial^2 \theta}{\partial y^2} \right) + Ec \left[\left(\frac{\partial u}{\partial y} + \delta^2 \frac{\partial v}{\partial x} \right)^2 + 2 \delta^2 \left(\frac{\partial u}{\partial x} \right)^2 + 2 \delta^2 \left(\frac{\partial v}{\partial y} \right)^2 \right] \quad 24$$

$$S_{xx} = 2(1+w) \frac{\partial u}{\partial x} - 2A \left[2\delta^2 \left(\frac{\partial u}{\partial x} \right)^2 + \left(\frac{\partial u}{\partial y} + \delta^2 \frac{\partial v}{\partial x} \right)^2 + 2\delta^2 \left(\frac{\partial v}{\partial y} \right)^2 \right] \frac{\partial u}{\partial x} \quad 25$$

$$S_{xy} = (1+w) \left(\delta^2 \frac{\partial v}{\partial x} + \frac{\partial u}{\partial y} \right) - A \left[2\delta^2 \left(\frac{\partial u}{\partial x} \right)^2 + \left(\frac{\partial u}{\partial y} + \delta^2 \frac{\partial v}{\partial x} \right)^2 + 2\delta^2 \left(\frac{\partial v}{\partial y} \right)^2 \right] \left(\delta^2 \frac{\partial v}{\partial x} + \frac{\partial u}{\partial y} \right) \quad 26$$

$$S_{yy} = 2(1+w) \left(\delta \frac{\partial v}{\partial y} \right) - 2A \delta \left[2\delta^2 \left(\frac{\partial u}{\partial x} \right)^2 + \left(\frac{\partial u}{\partial y} + \delta^2 \frac{\partial v}{\partial x} \right)^2 + 2\delta^2 \left(\frac{\partial v}{\partial y} \right)^2 \right] \quad 27$$

In previous equations, Pr is the Prandtl number, Ec is the Eckert number and θ is the dimensionless temperature.

Following are the relations between the stream function (Ψ) and velocity components:

$$u = \frac{\partial \Psi}{\partial y}, v = -\frac{\partial \Psi}{\partial x} \quad 28$$

Substituting Eq.28 into Eqs. 21 to 27, noting that the mass balance displayed by Eq.21 is similarly satisfied, produces the consequence that Eq.28 is satisfied.

$$Re \delta \left(\frac{\partial^2 \Psi}{\partial t \partial y} + \frac{\partial^3 \Psi}{\partial x \partial y^2} - \frac{\partial^3 \Psi}{\partial x \partial y^2} \right) - \frac{\rho d^2 \Omega}{\mu} \left(\Omega \frac{\partial \Psi}{\partial y} - 2 \frac{\delta c}{d} \frac{\partial^2 \Psi}{\partial t \partial x} \right) = -\frac{\partial p}{\partial x} + \delta^2 \frac{\partial}{\partial x} S_{xx} + \frac{\partial}{\partial y} S_{xy} - Ha^2 \cos \beta \left(\frac{\partial \Psi}{\partial y} \cos \beta + \delta \frac{\partial \Psi}{\partial x} \sin \beta \right) - \frac{1}{Da} \frac{\partial \Psi}{\partial y} + \frac{Re}{Fr} \sin \alpha^* \quad 29$$

$$Re \delta^3 \left(-\frac{\partial^2 \Psi}{\partial t \partial x} - \frac{\partial^3 \Psi}{\partial x^2 \partial y} - \frac{\partial^3 \Psi}{\partial x^2 \partial y} \right) - \frac{\rho d^2 \Omega \delta}{\mu} \left(\Omega \frac{\partial \Psi}{\partial x} - 2 \frac{\delta c}{d} \frac{\partial^2 \Psi}{\partial t \partial x} \right) = -\frac{\partial p}{\partial y} + \delta^2 \frac{\partial}{\partial x} S_{xy} + \delta \frac{\partial}{\partial y} S_{yy} + Ha^2 \sin \beta \left(\delta \frac{\partial \Psi}{\partial y} \cos \beta + \delta^2 \frac{\partial \Psi}{\partial x} \sin \beta \right) + \delta^2 \frac{1}{Da} \frac{\partial \Psi}{\partial x} + \delta \frac{Re}{Fr} \cos \alpha^* \quad 30$$

$$Re \delta \left(\frac{\partial \theta}{\partial t} + \frac{\partial \Psi}{\partial y} \frac{\partial \theta}{\partial x} - \frac{\partial \Psi}{\partial x} \frac{\partial \theta}{\partial y} \right) = \frac{1}{Pr} \left(c^2 \delta^2 \frac{\partial^2 \theta}{\partial t^2} + \delta^2 \frac{\partial^2 \theta}{\partial x^2} + \frac{\partial^2 \theta}{\partial y^2} \right) + Ec \left[\left(\frac{\partial^2 \Psi}{\partial y^2} + \delta^2 \frac{\partial^2 \Psi}{\partial x^2} \right)^2 + 2\delta^2 \left(\frac{\partial^2 \Psi}{\partial x \partial y} \right)^2 + 2\delta^2 \left(\frac{\partial^2 \Psi}{\partial x \partial y} \right)^2 \right] \quad 31$$

$$S_{xx} = 2(1+w) \frac{\partial^2 \Psi}{\partial x \partial y} - 2A \left[2\delta^2 \left(\frac{\partial^2 \Psi}{\partial x \partial y} \right)^2 + \left(\frac{\partial^2 \Psi}{\partial y^2} - \delta^2 \frac{\partial^2 \Psi}{\partial x^2} \right)^2 + 2\delta^2 \left(\frac{\partial^2 \Psi}{\partial x \partial y} \right)^2 \right] \quad 32$$

$$S_{xy} = (1+w) \left(-\delta^2 \frac{\partial^2 \Psi}{\partial x^2} + \frac{\partial^2 \Psi}{\partial y^2} \right) - A \left[2\delta^2 \left(\frac{\partial^2 \Psi}{\partial x \partial y} \right)^2 + \left(-\delta^2 \frac{\partial^2 \Psi}{\partial x^2} + \delta^2 \frac{\partial^2 \Psi}{\partial y^2} \right)^2 + 2\delta^2 \left(\frac{\partial^2 \Psi}{\partial x \partial y} \right)^2 \right] \left(-\delta^2 \frac{\partial^2 \Psi}{\partial x^2} + \frac{\partial^2 \Psi}{\partial y^2} \right) \quad 33$$

$$S_{yy} = -2(1+w) \delta \frac{\partial^2 \Psi}{\partial x \partial y} - 2A \delta \left[2\delta^2 \left(\frac{\partial^2 \Psi}{\partial x \partial y} \right)^2 + \left(\frac{\partial^2 \Psi}{\partial y^2} - \delta^2 \frac{\partial^2 \Psi}{\partial x^2} \right)^2 + 2\delta^2 \left(\frac{\partial^2 \Psi}{\partial x \partial y} \right)^2 \right] \left(-\frac{\partial^2 \Psi}{\partial x \partial y} \right) \quad 34$$

Now, Eqs.29- 34 become the form when (*Re* and $\delta \ll 1$) are present:

While the component of the extra stress tensor becomes the form of

Also, if Eq.39 is entered into Eq.35 as well as the derivative with regard to *y* and by (*w*+1) is taken, then the following equation is obtained:

$$-\frac{\rho d^2 \Omega^2}{\mu} \frac{\partial \Psi}{\partial y} = -\frac{\partial p}{\partial x} + \frac{\partial}{\partial y} S_{xy} - \left(Ha^2 \cos^2 \beta + \frac{1}{Da} \right) \frac{\partial \Psi}{\partial y} + \frac{Re}{Fr} \sin \alpha^* \quad 35$$

$$-\frac{\partial p}{\partial y} = 0 \quad 36$$

$$\frac{\partial^2 \theta}{\partial y^2} = -Ec.Pr \left(\frac{\partial^2 \Psi}{\partial y^2} \right)^2 \quad 37$$

$$S_{xx} = 2(1+w) \frac{\partial^2 \Psi}{\partial x \partial y} - 2A \left(\frac{\partial^2 \Psi}{\partial y^2} \right)^2 \frac{\partial^2 \Psi}{\partial x \partial y} \quad 38$$

$$S_{xy} = (1+w) \left(\frac{\partial^2 \Psi}{\partial y^2} \right) - A \left(\frac{\partial^2 \Psi}{\partial y^2} \right)^3 \quad 39$$

$$S_{yy} = 0 \quad 40$$

Where

$$\zeta = \frac{Ha^2 \cos^2 \beta + \frac{1}{Da} - \frac{\rho d^2 \Omega^2}{\mu}}{w+1}, \quad \eta = \frac{1}{w+1}$$

In the wave frame, the dimensionless volume flow rate and boundary condition are as follows: *F* represents the dimensionless temporal average flow in the wave frame.

$$\Psi = \frac{F}{2}, \quad \frac{\partial \Psi}{\partial y} = -1, \quad \theta = 0 \quad \text{at } y = h_1 \quad 42$$

$$\Psi = -\frac{F}{2}, \quad \frac{\partial \Psi}{\partial y} = -1, \quad \theta = 0 \quad \text{at } y = h_2 \quad 43$$

Problem's Resolution

A non-linear system of partial differential equations is solved using the perturbation method by increasing flow amounts in a power series of *A*.

$$\Psi = \Psi_0 + A\Psi_1 + O(A^2) \quad 44$$

$$P = P_0 + AP_1 + O(A^2) \quad 45$$

Now, by substituting Eqs.44 – 45 into Eqs.35 – 40 and boundary conditions (42), (43) and comparing the coefficients of the same *A* power up to the first order yields the two system solutions listed below:

1. Zeroth Order System

When the terms of order (*A*) in a zeroth-order system are negligible, then

$$\Psi_{0yyyy} - \zeta \Psi_{0yy} = 0 \quad 46$$

Such is the case

$$\Psi_0 = \frac{F_0}{2}, \quad \frac{\partial \Psi_0}{\partial y} = -1 \quad \text{at } y = h_1 \quad 47$$

and

$$\Psi_0 = -\frac{F_0}{2}, \quad \frac{\partial \Psi_0}{\partial y} = -1 \quad \text{at } y = h_2 \quad 48$$

2. First Order System

$$\Psi_{1yyyy} - \eta \frac{\partial^2}{\partial y^2} (\Psi_{0yy})^3 - \zeta \Psi_{1yy} = 0 \quad 49$$

$$\Psi_{1yyyy} - \zeta \Psi_{1yy} = \eta \frac{\partial^2}{\partial y^2} (\Psi_{0yy})^3 \quad 50$$

$$\Psi_1 = \frac{F_1}{2}, \quad \frac{\partial \Psi_1}{\partial y} = 0 \quad \text{at } y = h_1 \quad 51$$

and

$$\Psi_1 = -\frac{F_1}{2}, \quad \frac{\partial \Psi_1}{\partial y} = 0 \quad \text{at } y = h_2 \quad 52$$

Solving associated zeroth and first-order systems yields the final equation for the stream function.

$$\Psi = \Psi_0 + A\Psi_1 \quad 53$$

$$\Psi = \frac{e^{-\gamma\sqrt{\zeta}}(e^{2\gamma\sqrt{\zeta}}c_1+c_2)}{\zeta} + c_3 + \gamma c_4 +$$

$$A[(e^{-3\gamma\sqrt{\zeta}}(e^{3(h_1+h_2)\sqrt{\zeta}}(F_0+h_1-h_2)^3\zeta^3\eta - e^{6\gamma\sqrt{\zeta}}(F_0+h_1-h_2)^3\zeta^3\eta +$$

$$\begin{aligned}
 &6e^{(h_1+h_2+4y)\sqrt{\zeta}}(F_0 + h_1 - h_2)^3(-5 + \\
 &2y\sqrt{\zeta})\zeta^3\eta + 6e^{2(h_1+h_2+y)\sqrt{\zeta}}(F_0 + h_1 - h_2)^3(5 + \\
 &2y\sqrt{\zeta})\zeta^3\eta + 8e^{(3h_1+4y)\sqrt{\zeta}}(-2 + h_1\sqrt{\zeta} - \\
 &h_2\sqrt{\zeta})^3A_1 + 24e^{(h_1+2h_2+4y)\sqrt{\zeta}}(-2 + h_1\sqrt{\zeta} - \\
 &h_2\sqrt{\zeta})(2 + h_1\sqrt{\zeta} - h_2\sqrt{\zeta})^2A_1 - \\
 &8e^{(3h_2+4y)\sqrt{\zeta}}(-2 - h_1\sqrt{\zeta} + h_2\sqrt{\zeta})^3A_1 + \\
 &24e^{(2h_1+h_2+4y)\sqrt{\zeta}}(2 + h_1\sqrt{\zeta} - h_2\sqrt{\zeta})(2 - \\
 &h_1\sqrt{\zeta} + h_2\sqrt{\zeta})^2A_1 + 8e^{(3h_1+2y)\sqrt{\zeta}}(-2 + h_1\sqrt{\zeta} - \\
 &h_2\sqrt{\zeta})^3A_2 + 24e^{(h_1+2(h_2+y))\sqrt{\zeta}}(-2 + h_1\sqrt{\zeta} - \\
 &h_2\sqrt{\zeta})(2 + h_1\sqrt{\zeta} - h_2\sqrt{\zeta})^2A_2 - \\
 &8e^{(3h_2+2y)\sqrt{\zeta}}(-2 - h_1\sqrt{\zeta} + h_2\sqrt{\zeta})^3A_2 + \\
 &24e^{(2h_1+h_2+2y)\sqrt{\zeta}}(2 + h_1\sqrt{\zeta} - h_2\sqrt{\zeta})(2 - \\
 &h_1\sqrt{\zeta} + h_2\sqrt{\zeta})^2A_2)/[8(e^{h_1\sqrt{\zeta}}(-2 + h_1\sqrt{\zeta} - \\
 &h_2\sqrt{\zeta}) + e^{h_2\sqrt{\zeta}}(2 + h_1\sqrt{\zeta} - h_2\sqrt{\zeta}))^3\zeta] + A_3 + \\
 &yA_4] \quad 54
 \end{aligned}$$

Results and Discussion

This section consists of two subsections. In the first, the pressure gradient is discussed, while in the second, the temperature distribution is illustrated using the MATHEMATICA software.

❖ Pressure Gradient dp/dx :

Case variation of dp/dx indicates the variance in the axial pressure gradient across the channel. The influence of various values (Ha , β , Da , Ω , w , ϕ , A , Fr , Re , α^*) on the axial pressure gradient dp/dx is illustrated in Figs. 2 - 11

- Figs. 2 and 8 demonstrate that increases in the values of the Hartman number (Ha) and the material fluid parameter (A) cause the axial pressure gradient to decrease as the curve's vertex, but have no effect on the axial pressure gradient near the right or left channel wall.
- In Figs. 3 and 4, the increases in the values of Darcy number (Da) and the inclination of the magnetic field (β) lead to the axial pressure gradient increasing as the vertex of the curve is twisted to the right but the axial pressure gradient close to the right or left walls of the channel is unaffected, while in Fig.6 the increases in the values of the porous medium parameter (w) lead to the axial pressure gradient increases as the vertex of the curve only but the axial pressure

Within the fixed frame, the axial velocity component is expressed as

$$u(x, y, t) = \Psi_y \quad 55$$

It is possible to rewrite Eq.35 as

$$\begin{aligned}
 \frac{\partial p}{\partial x} &= \Psi_{0yyy} - \zeta\Psi_{0y} + A\Psi_{1yyy} - \\
 \eta A \frac{\partial}{\partial y} (\Psi_{0yy})^3 &- A\zeta\Psi_{1yy} \quad 56
 \end{aligned}$$

Energy Equation Solution

The long wavelength and low Reynolds approximation are used to get Eq. 37.

$$\frac{1}{Pr} \left(\frac{\partial^2 \theta}{\partial y^2} \right) + Ec \left(\frac{\partial^2 \Psi}{\partial y^2} \right)^2 = 0 \quad 57$$

The solution of Eq.57 with boundary conditions

$$\theta = 0 \text{ at } y = h_1 \text{ and } \theta = 1 \text{ at } y = h_2 \quad 58$$

It is possible to prove that r_1 and r_2 are constants using the boundary conditions, and can be stated θ as in the index.

gradient close to the right or left walls of the channel is unaffected.

- Figs. 5, 9, 10, and 11 demonstrate that the axial pressure gradient does not change as the rotation (Ω), the Froude number (Fr), the Reynolds number (Re), and the inclination angle of the channel to the horizontal axis (α^*) values increase.
- In Fig. 7, for approximately $-1.9 < x < 0$, and $-2.8 < x < -2.2$, the axial velocity increases as the amplitude ratio increases (ϕ), but for approximately $-4 < x < -2.8$, the axial pressure gradient decreases slightly. However, for $-2.2 < x < -1.9$ and $0 < x < 1$, the axial pressure does not change.

❖ Temperature Distribution θ :

The effect of relevant parameters on the temperature distribution θ is graphically illustrated in Figs. 12 - 21 whereas depicted in the following figures, the behavior of temperature distribution is parabolic.

- Figs. 12, 17, 18, 19, and 20 illustrate that increases in the values of the Hartman number (Ha), the amplitude ratio (ϕ), the material fluid parameter (A), the Eckert number (Ec), and the

Prandtl number (Pr) have no effect on the temperature field in the channel's central region, whereas the temperature field decreases near the channel wall.

- Figs. 13, 14, 15, and 16 display the increases in the values of Darcy number (Da), the inclination of the magnetic field (β), the rotation (Ω), and porous medium parameter (w) there is no effect on the temperature field in the central region of the channel, whereas the temperature field is rising close to the channel wall's margin.
- The temperature field does not change as the Reynolds number (Re), the Froude number (Fr), and the inclination angle of the channel to the horizontal axis (α^*) values increase, as shown in Figs. 21, 22, and 23.

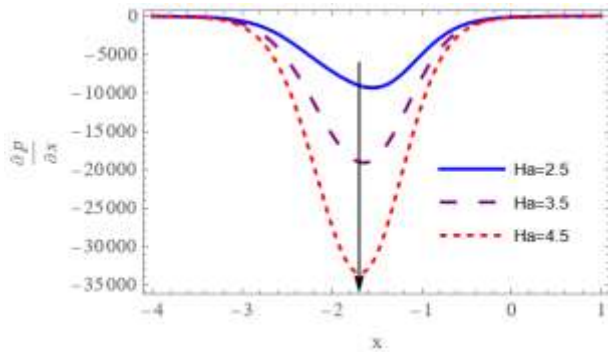


Figure 2. Pressure gradient variation for different (Ha) values when $\beta = 0.1$, $Da = 0.2$, $\rho = 0$, $d = 0.5$, $\Omega = 0.2$, $\mu = 3$, $w = 0.3$, $\phi = 0.2$, $a = 0.2$, $b = 0.2$, $d_1 = 0.5$, $F_0 = 0.4$, $F_1 = 0$, $A = 0.3$, $Fr = 0.7$, $Re = 0.2$, $\alpha^* = 0.5$

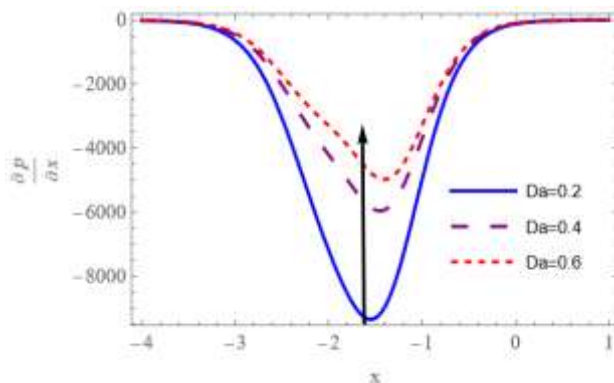


Figure 3. Pressure gradient variation for different (Da) values when $Ha = 2.5$, $\beta = 0.1$, $\rho = 0.1$, $d = 0.5$, $\Omega = 0.2$, $\mu = 3$, $w = 0.3$, $\phi = 0.2$, $a = 0.2$, $b = 0.2$, $d_1 = 0.5$, $F_0 = 0.4$, $F_1 = 0$, $A = 0.3$, $Fr = 0.7$, $Re = 0.2$, $\alpha^* = 0.5$

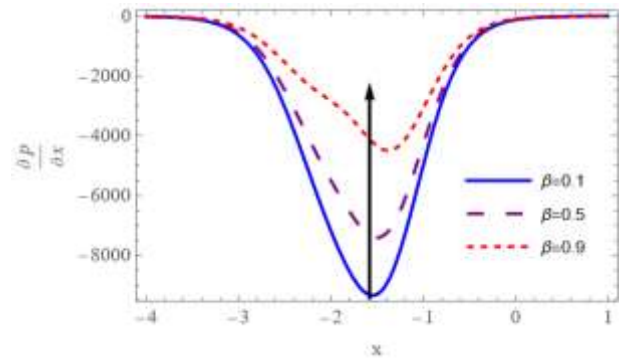


Figure 4. Pressure gradient variation for different (β) values when $Ha = 2.5$, $Da = 0.2$, $\rho = 0.1$, $d = 0.5$, $\Omega = 0.2$, $\mu = 3$, $w = 0.3$, $\phi = 0.2$, $a = 0.2$, $b = 0.2$, $d_1 = 0.5$, $F_0 = 0.4$, $F_1 = 0$, $A = 0.3$, $Fr = 0.7$, $Re = 0.2$, $\alpha^* = 0.5$

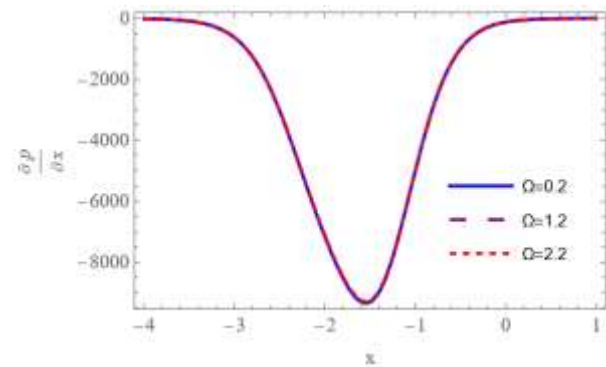


Figure 5. Pressure gradient variation for different (Ω) values when $Ha = 2.5$, $\beta = 0.1$, $Da = 0.2$, $\rho = 0.1$, $d = 0.5$, $\mu = 3$, $w = 0.3$, $\phi = 0.2$, $a = 0.2$, $b = 0.2$, $d_1 = 0.5$, $F_0 = 0.4$, $F_1 = 0$, $A = 0.3$, $Fr = 0.7$, $Re = 0.2$, $\alpha^* = 0.5$

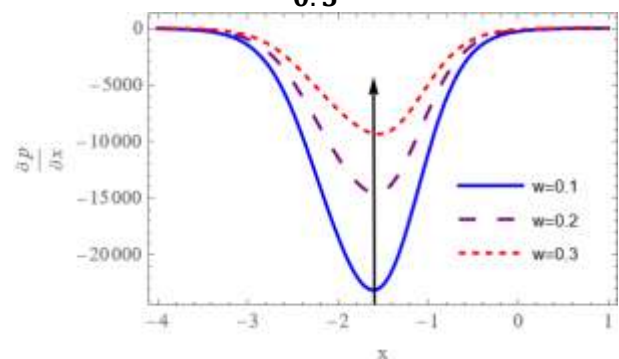


Figure 6. Pressure gradient variation for different (w) values when $Ha = 2.5$, $\beta = 0.1$, $Da = 0.2$, $\rho = 0.1$, $d = 0.5$, $\Omega = 0.2$, $\mu = 3$, $\phi = 0.2$, $a = 0.2$, $b = 0.2$, $d_1 = 0.5$, $F_0 = 0.4$, $F_1 = 0$, $A = 0.3$, $Fr = 0.7$, $Re = 0.2$, $\alpha^* = 0.5$

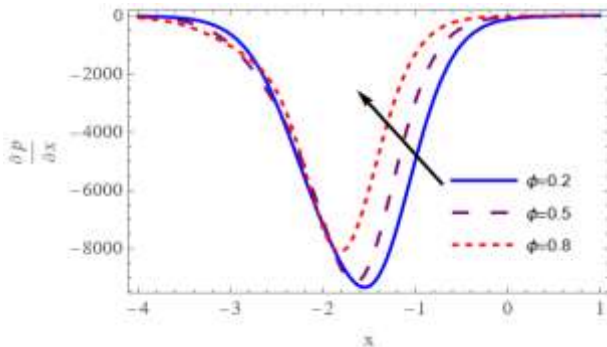


Figure 7. Pressure gradient variation for different (ϕ) values when $Ha = 2.5, \beta = 0.1, Da = 0.2, \rho = 0.1, d = 0.5, \Omega = 0.2, \mu = 3, w = 0.3, a = 0.2, b = 0.2, d_1 = 0.5, F_0 = 0.4, F_1 = 0, A = 0.3, Fr = 0.7, Re = 0.2, \alpha^* = 0.5$

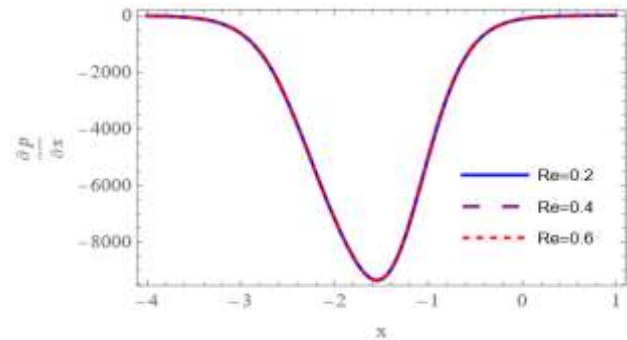


Figure 10. Pressure gradient variation for different (Re) values when $Ha = 2.5, \beta = 0.1, Da = 0.2, \rho = 0.1, d = 0.5, \Omega = 0.2, \mu = 3, w = 0.3, \phi = 0.2, a = 0.2, b = 0.2, d_1 = 0.5, F_0 = 0.4, F_1 = 0, A = 0.3, Fr = 0.7, \alpha^* = 0.5$

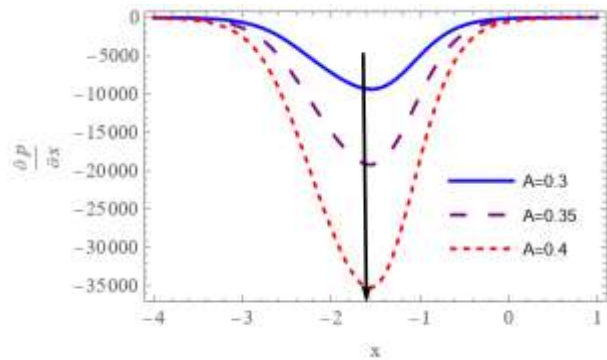


Figure 8. Pressure gradient variation for different (A) values when $Ha = 2.5, \beta = 0.1, Da = 0.2, \rho = 0.1, d = 0.5, \Omega = 0.2, \mu = 3, w = 0.3, \phi = 0.2, a = 0.2, b = 0.2, d_1 = 0.5, F_0 = 0.4, F_1 = 0, A = 0.3, Re = 0.2, \alpha^* = 0.5$

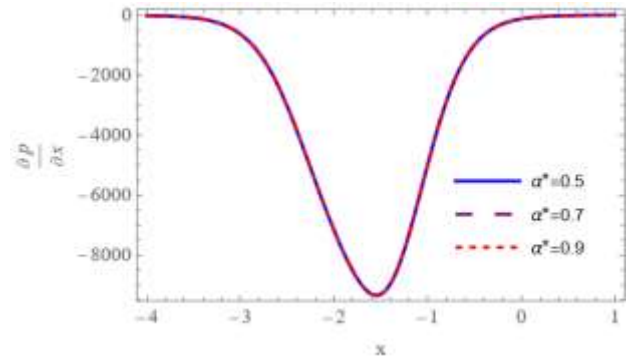


Figure 11. Pressure gradient variation for different (α^*) values when $Ha = 2.5, \beta = 0.1, Da = 0.2, \rho = 0.1, d = 0.5, \Omega = 0.2, \mu = 3, w = 0.3, \phi = 0.2, a = 0.2, b = 0.2, d_1 = 0.5, F_0 = 0.4, F_1 = 0, A = 0.3, Fr = \alpha^* 0.7, Re = 0.2$

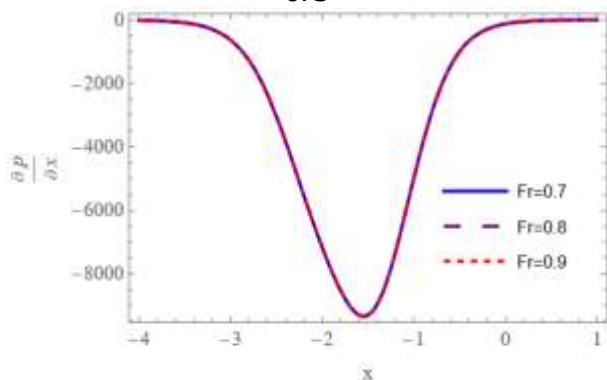


Figure 9. Pressure gradient variation for different (Fr) values when $Ha = 2.5, \beta = 0.1, Da = 0.2, \rho = 0.1, d = 0.5, \Omega = 0.2, \mu = 3, w = 0.3, \phi = 0.2, a = 0.2, b = 0.2, d_1 = 0.5, F_0 = 0.4, F_1 = 0, A = 0.3, Re = 0.2, \alpha^* = 0.5$

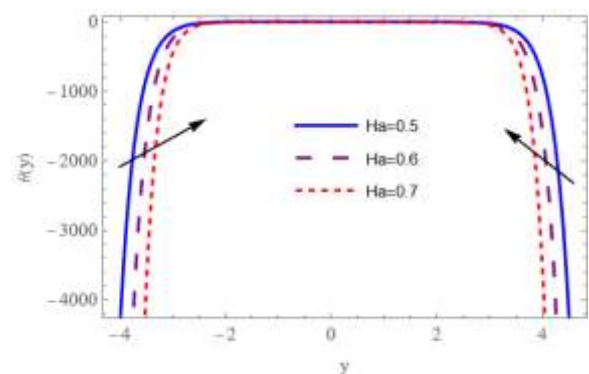


Figure 12. Temperature variation for various (Ha) values when $Ha = 0.5, \beta = 0.1, Da = 10, \rho = 0.1, d = 0.5, \Omega = 0.5, \mu = 3, w = 0.3, \phi = 1.3, a = 0.2, b = 0.2, d_1 = 0.5, F_0 = 0.4, F_1 = 0, A = 0.1, Ec = 0.05, Pr = 0.05, Re = 2, Fr = 1, \alpha^* = 1.5$

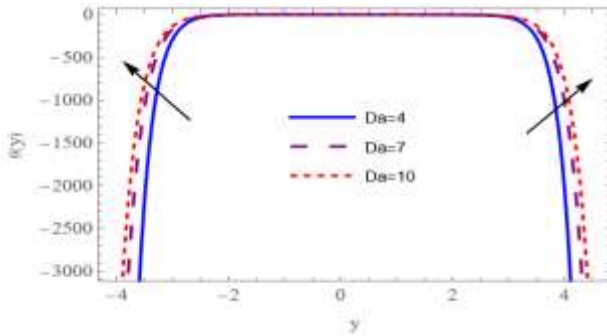


Figure 13. Temperature variation for various (Da) values when $Ha = 0.5, \beta = 0.1, Da = 10, \rho = 0.1, d = 0.5, \Omega = 0.5, \mu = 3, w = 0.3, \phi = 1.3, a = 0.2, b = 0.2, d_1 = 0.5, F_0 = 0.4, F_1 = 0, A = 0.1, Ec = 0.05, Pr = 0.05, Re = 2, Fr = 1, \alpha^* = 1.5$

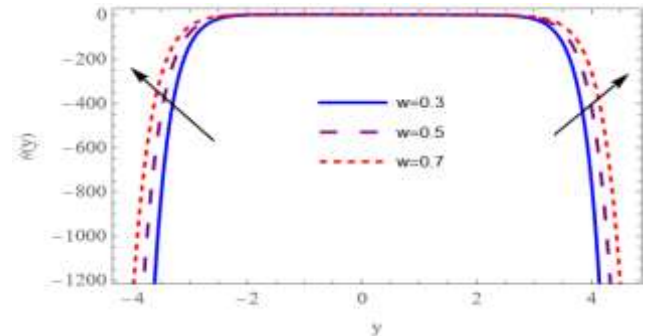


Figure 16. Temperature variation for various (w) values when $Ha = 0.5, \beta = 0.1, Da = 10, \rho = 0.1, d = 0.5, \Omega = 0.5, \mu = 3, w = 0.3, \phi = 1.3, a = 0.2, b = 0.2, d_1 = 0.5, F_0 = 0.4, F_1 = 0, A = 0.1, Ec = 0.05, Pr = 0.05, Re = 2, Fr = 1, \alpha^* = 1.5$

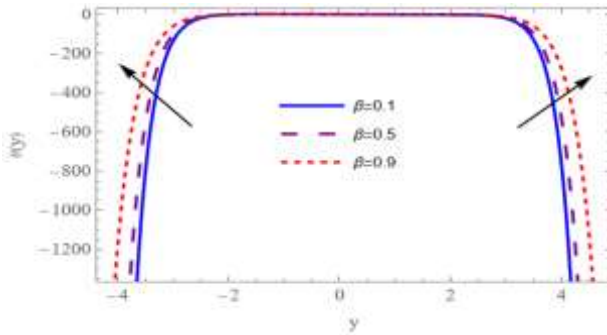


Figure 14. Temperature variation for various (β) values when $Ha = 0.5, \beta = 0.1, Da = 10, \rho = 0.1, d = 0.5, \Omega = 0.5, \mu = 3, w = 0.3, \phi = 1.3, a = 0.2, b = 0.2, d_1 = 0.5, F_0 = 0.4, F_1 = 0, A = 0.1, Ec = 0.05, Pr = 0.05, Re = 2, Fr = 1, \alpha^* = 1.5$

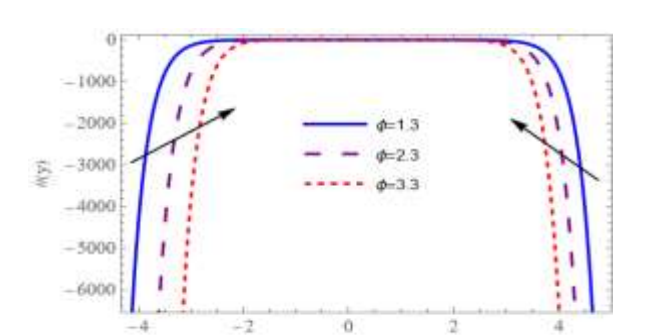


Figure 17. Temperature variation for various (ϕ) values when $Ha = 0.5, \beta = 0.1, Da = 10, \rho = 0.1, d = 0.5, \Omega = 0.5, \mu = 3, w = 0.3, \phi = 1.3, a = 0.2, b = 0.2, d_1 = 0.5, F_0 = 0.4, F_1 = 0, A = 0.1, Ec = 0.05, Pr = 0.05, Re = 2, Fr = 1, \alpha^* = 1.5$

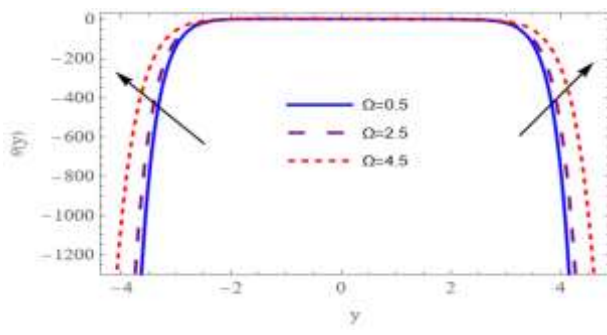


Figure 15. Temperature variation for various (Ω) values when $Ha = 0.5, \beta = 0.1, Da = 10, \rho = 0.1, d = 0.5, \Omega = 0.5, \mu = 3, w = 0.3, \phi = 1.3, a = 0.2, b = 0.2, d_1 = 0.5, F_0 = 0.4, F_1 = 0, A = 0.1, Ec = 0.05, Pr = 0.05, Re = 2, Fr = 1, \alpha^* = 1.5$

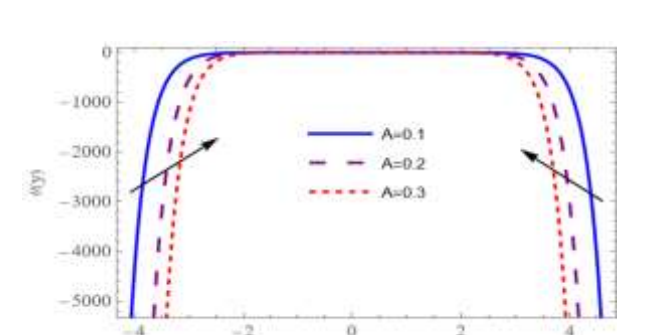


Figure 18. Temperature variation for various (A) values when $Ha = 0.5, \beta = 0.1, Da = 10, \rho = 0.1, d = 0.5, \Omega = 0.5, \mu = 3, w = 0.3, \phi = 1.3, a = 0.2, b = 0.2, d_1 = 0.5, F_0 = 0.4, F_1 = 0, A = 0.1, Ec = 0.05, Pr = 0.05, Re = 2, Fr = 1, \alpha^* = 1.5$

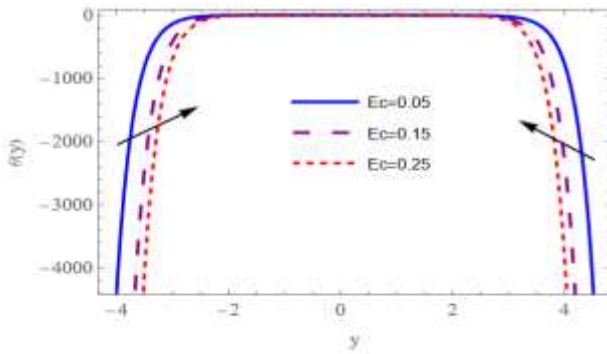


Figure 19. Temperature variation for various (Ec) values when $Ha = 0.5, \beta = 0.1, Da = 10, \rho = 0.1, d = 0.5, \Omega = 0.5, \mu = 3, w = 0.3, \phi = 1.3, a = 0.2, b = 0.2, d_1 = 0.5, F_0 = 0.4, F_1 = 0, A = 0.1, Ec = 0.05, Pr = 0.05, Re = 2, Fr = 1, \alpha^* = 1.5$

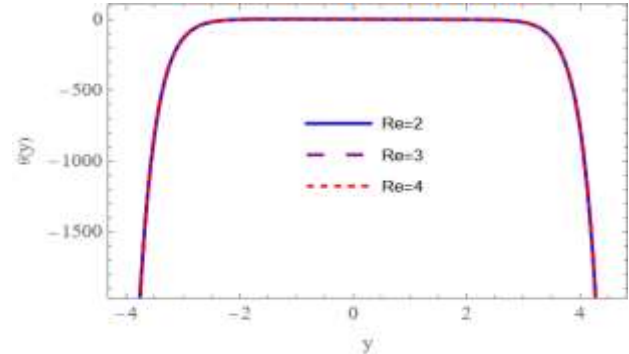


Figure 21. Temperature variation for various (Re) values when $Ha = 0.5, \beta = 0.1, Da = 10, \rho = 0.1, d = 0.5, \Omega = 0.5, \mu = 3, w = 0.3, \phi = 1.3, a = 0.2, b = 0.2, d_1 = 0.5, F_0 = 0.4, F_1 = 0, A = 0.1, Ec = 0.05, Pr = 0.05, Re = 2, Fr = 1, \alpha^* = 1.5$

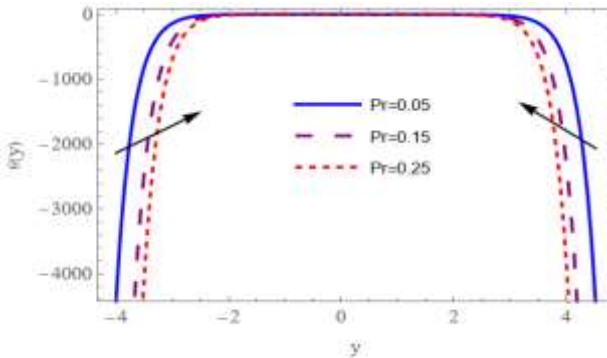


Figure 20. Temperature variation for various (Pr) values when $Ha = 0.5, \beta = 0.1, Da = 10, \rho = 0.1, d = 0.5, \Omega = 0.5, \mu = 3, w = 0.3, \phi = 1.3, a = 0.2, b = 0.2, d_1 = 0.5, F_0 = 0.4, F_1 = 0, A = 0.1, Ec = 0.05, Pr = 0.05, Re = 2, Fr = 1, \alpha^* = 1.5$

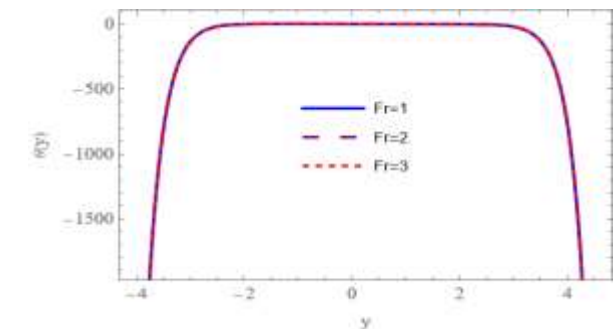


Figure 22. Temperature variation for various (Fr) values when $Ha = 0.5, \beta = 0.1, Da = 10, \rho = 0.1, d = 0.5, \Omega = 0.5, \mu = 3, w = 0.3, \phi = 1.3, a = 0.2, b = 0.2, d_1 = 0.5, F_0 = 0.4, F_1 = 0, A = 0.1, Ec = 0.05, Pr = 0.05, Re = 2, Fr = 1, \alpha^* = 1.5$

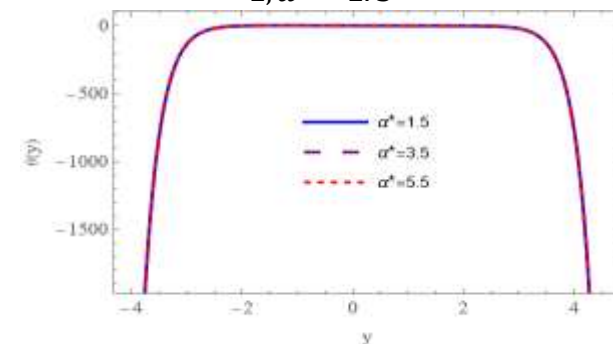


Figure 23. Temperature variation for various (α^*) values when $Ha = 0.5, \beta = 0.1, Da = 10, \rho = 0.1, d = 0.5, \Omega = 0.5, \mu = 3, w = 0.3, \phi = 1.3, a = 0.2, b = 0.2, d_1 = 0.5, F_0 = 0.4, F_1 = 0, A = 0.1, Ec = 0.05, Pr = 0.05, Re = 2, Fr = 1, \alpha^* = 1.5$

Conclusion

In this study, the rotational effects of peristaltic transport of a Powell-Eyring fluid in an asymmetric channel through a porous material susceptible to the combined acts of inclined MHD are investigated. The asymmetric channel is formed by selecting peristaltic waves with varying amplitudes and phases on the non-uniform walls and a low Reynolds number. Using the perturbation approach, the formulas for the axial velocity and pressure gradient are produced. Multiple graphs are utilized for parameter analysis:

I) When the values of Hartman number (Ha) and material fluid parameter (A) increase, the axial pressure gradient decreases as the vertex of the curve is twisted to the right. However, the axial pressure gradient close to the right or left walls of the channel is unaffected. However, the opposite occurs when the values of Darcy number (Da), and the inclination of magnetic field (β) increase, while the increases in the values of the porous medium parameter (w) lead to the axial pressure gradient increases as the vertex of the curve only while demonstrating that the axial pressure gradient does not change as the rotation (Ω), the Froude number (Fr), the Reynolds number (Re),

and the inclination angle of the channel to the horizontal axis (α^*) values increase. Whereas for approximately $-1.9 < x < 0$, and $-2.8 < x < -2.2$, the axial velocity increases as the amplitude ratio increases (ϕ), but for approximately $-4 < x < -2.8$, the axial pressure gradient decreases slightly. However, for $-2.2 < x < -1.9$ and $0 < x < 1$, the axial pressure does not change.

II) As the Hartman number (Ha), the amplitude ratio (ϕ), material fluid parameter (A), Eckert number (Ec), and Prandtl number (Pr) increases, the temperature field decreases in the vicinity of the channel's wall but no change in the channel's central region, while the increases in the values of Darcy number (Da), the inclination of magnetic field (β), the rotation (Ω), and porous medium parameter (w) there is no effect on the temperature field in the channel's central region, the temperature field increases in the vicinity of the channel's wall and furthermore increasing values of Reynolds number (Re), Froude number (Fr), and inclination angle of the channel to the horizontal axis (α^*) have no effect on the temperature field.

Authors' Declaration

- Conflicts of Interest: None.
- We hereby confirm that all the Figures and Tables in the manuscript are ours. Furthermore, any Figures and images, that are not ours, have been

- included with the necessary permission for re-publication, which is attached to the manuscript.
- Ethical Clearance: The project was approved by the local ethical committee in University of Baghdad.

Authors' Contribution Statement

This work was carried out in collaboration between both authors. R. Gh. I. and L. Z. H. read and approved the final manuscript.

References

1. Latham TW. Fluid Motion in Peristaltic Pumps. USA: Massachusetts Institute of Technology, Cambridge; 1966. <https://dspace.mit.edu/handle/1721.1/17282>
2. Hina S, Mustafa M, Hayat T, Alsaedi A. Peristaltic Flow of Powell-Eyring Fluid in Curved Channel with Heat Transfer: A Useful Application in Biomedicine. *Comput Methods Programs Biomed.* 2016 ;135: 89–100. <https://doi.org/10.1016/j.cmpb.2016.07.019>.
3. Hayat T, Aslam N, Rafiq M, Alsaadi FE. Hall and Joule Heating Effects on Peristaltic Flow of Powell-Eyring Liquid in an Inclined Symmetric Channel. *Results Phys.* 2017; 7: 518–28. <https://doi.org/10.1016/j.rinp.2017.01.008>.
4. Ali HA, Abdulhadi AM. Analysis of Heat Transfer on Peristaltic Transport of Powell-Eyring Fluid in an Inclined Tapered Symmetric Channel with Hall and Ohm's Heating Influences. *J AL-Qadisiyah Comput Sci Math.* 2018; 10(2): 26-41. <https://doi.org/10.29304/jqcm.2018.10.2.364>.
5. Hussain Q, Alvi N, Latif T, Asghar S. Radiative Heat



- Transfer in Powell–Eyring Nanofluid with Peristalsis. *Int J Thermophys.* 2019; 40(5): 1–20. <https://doi.org/10.1007/s10765-019-2510-8>.
6. Hummady LZ. Effect of Couple Stress on Peristaltic Transport of Powell-Eyring Fluid Peristaltic Flow in Inclined Asymmetric Channel with Porous Medium. *Wasit J Comput Math Sci.* 2022; 1(2): 106–18. <https://doi.org/10.31185/wjcm.Vol1.Iss2.31>.
 7. Satya Narayana P V, Tarakaramu N, Moliya Akshit S, Ghori J. MHD Flow and Heat Transfer of an Eyring-Powell Fluid over a Linear Stretching Sheet with Viscous Dissipation-A Numerical Study. *Front. Heat Mass Transf.* 2017; 9(1): 66–71. <http://dx.doi.org/10.5098/hmt.9.9>.
 8. Eldabe NT, Kamel KA, Ramadan SF, Saad RA. Peristaltic Motion of Eyring-Powell Nanofluid with Couple Stresses and Heat and Mass Transfer Through a Porous Media under the Effect of Magnetic Field Inside Asymmetric Vertical Channel. *J Adv Res Fluid Mech Therm Sci.* 2020;68(2):58–71. <https://doi.org/10.37934/arfmts.68.2.5871>.
 9. Noreen S, Kausar T, Tripathi D, Ain QU, Lu DC. Heat Transfer Analysis on Creeping Flow Carreau Fluid Driven by Peristaltic Pumping in an Inclined Asymmetric Channel. *Therm Sci Eng Prog.* 2020; 17: 100486. <https://doi.org/10.1016/j.tsep.2020.100486>.
 10. Khudair WS, Dwail HH. Studying the Magnetohydrodynamics for Williamson Fluid with Varying Temperature and Concentration in an Inclined Channel with Variable Viscosity. *Baghdad Sci J.* 2021; 18(3) :531. <https://doi.org/10.21123/bsj.2021.18.3.0531>.
 11. Al-Khafajy DGS. Influence of Varying Temperature and Concentration on Magnetohydrodynamics Peristaltic Transport for Jeffrey Fluid with a Nanoparticles Phenomenon through a Rectangular Porous Duct. *Baghdad Sci J.* 2021;18(2):0279. <https://doi.org/10.21123/bsj.2021.18.2.0279>.
 12. Ahmed TS. Effect of Inclined Magnetic Field on Peristaltic Flow of Carreau Fluid through Porous Medium in an Inclined Tapered Asymmetric Channel. *Al-Mustansiriyah J Sci.* 2018;29(3):94–105. <http://doi.org/10.23851/mjs.v29i3.641>.
 13. Jasim AM. Study of the Impact of Unsteady Squeezing Magnetohydrodynamics Copper-Water with Injection-Suction on Nanofluid Flow Between Two Parallel Plates in Porous Medium. *Iraqi J Sci.* 2022; 63(9): 3909–3924. <https://doi.org/10.24996/ijs.2022.63.9.23>
 14. Ali HA. Impact of Varying Viscosity with Hall Current on Peristaltic Flow of Viscoelastic Fluid Through Porous Medium in Irregular Microchannel. *Iraqi J Sci.* 2022; 63(3): 1265–1276. <https://doi.org/10.24996/ijs.2022.63.3.31>
 15. Aziz A, Jamshed W, Aziz T, Bahaidarah HMS, Ur Rehman K. Entropy Analysis of Powell–Eyring Hybrid Nanofluid Including Effect of Linear Thermal Radiation and Viscous Dissipation. *J Therm Anal Calorim.* 2021; 143(2): 1331–43. <https://doi.org/10.1007/s10973-020-10210-2>
 16. Kareem RS, Abdulhadi AM. Impacts of Heat and Mass Transfer on Magneto Hydrodynamic Peristaltic Flow Having Temperature-Dependent Properties in an Inclined Channel Through Porous Media. *Iraqi J Sci.* 2020; 61(4): 854–869. <https://doi.org/10.24996/ijs.2020.61.4.19>
 17. Hage AK, Hummady LZ. Influence of Inclined Magnetic Field and Heat Transfer on Peristaltic Transfer Powell-Eyring Fluid in Asymmetric Channel and Porous Medium. *Int J Nonlinear Anal Appl.* 2022; 13(2): 631-642. https://ijnaa.semnan.ac.ir/article_6469_c684e6aed8053b7db3200ec3e9dbec56.pdf
 18. Mohaisen HN, Abedulhadi AM. Effects of the Rotation on the Mixed Convection Heat Transfer Analysis for the Peristaltic Transport of Viscoplastic Fluid in Asymmetric Channel. *Iraqi J Sci.* 2022; 63(3): 1240–1257. <https://doi.org/10.24996/ijs.2022.63.3.29>

تأثير المعلمات المختلفة على التدفق التمعجي لسائل باول آرينغ مع تأثير الدوران والانتقال الحراري في قناة غير متماثلة مائلة

رنا غازي ابراهيم¹، لقاء زكي حمادي²

قسم الرياضيات، كلية العلوم، جامعة بغداد، بغداد، العراق.

الخلاصة

في هذه المقالة، يتم فحص تأثير متغير الدوران والمتغيرات الأخرى على التدفق التمعجي لسائل Powell-Eyring في قناة غير متماثلة مائلة مع مجال مغناطيسي مائل عبر وسط مسامي مع نقل الحرارة. يُفترض الطول الموجي الطويل وعدد رينولدز المنخفض، حيث يتم استخدام نهج الاضطراب لحل المعادلات الحاكمة غير الخطية في نظام الإحداثيات الديكارتية لإنتاج حلول متسلسلة. يتم التعبير عن توزيعات السرعة وتدرجات الضغط رياضياً. من خلال جمع الأرقام، يتم شرح تأثير المعايير المختلفة وتمثيلها بيانياً. تم الحصول على هذه النتائج العددية باستخدام التطبيق الرياضي MATHEMATICA.

الكلمات المفتاحية: انتقال الحرارة، قناة المائلة، مجال مغناطيسي، تدفق تمعجي، وسط مسامي، سائل باول آرينغ، الدوران.